Progress In Electromagnetics Research M, Vol. 12, 181–192, 2010

INVESTIGATION OF ELECTROMAGNETIC SHIELDING ROOMS WITH METAL CABINET AND APERTURE

S. M. J. Razavi and M. Khalaj-Amirhosseini

College of Electrical Engineering
Iran University of Science and Technology
Tehran, Iran

Abstract—In this paper, a fast and efficient method has been proposed to analyze the electromagnetic shielding rooms with electrical large sizes and arbitrary shapes. The ray-tracing method is used to predict the Shielding Effectiveness (SE) of the electromagnetic shielding rooms. The proposed method is based on speeding up the ray tracing algorithm. The performance of the proposed method is verified by a comprehensive example. The effect of additional metal cabinet in the shielding effectiveness of shielding room has been investigated. Also the position of it has been found optimally to produce a "best" performance for the shielding room.

1. INTRODUCTION

Electromagnetic shielding is one of the standard approaches that reduces emissions or improves the immunity. The ability of an enclosure to do this is characterized by its shielding effectiveness (SE), defined as the ratio of field strengths in the presence and absence of the enclosure. The efficiency of shielding enclosures is compromised by the wall of the enclosure, slots and apertures for heat dissipation, cable penetration, peripherals and displays.

Shielding effectiveness can be calculated by numerical simulation or by analytical formulations. Numerical methods that have been used to calculate shielding effectiveness include transmission-line modeling (TLM) [1], finite-difference time-domain (FDTD) method [2], and the method of moments (MOM) [3]. Analytical formulation provides a much faster means of calculating shielding effectiveness, enabling the effect of design parameters to be investigated. Many of these are derived from Bethe's approximation of diffraction through holes [4]

Corresponding author: S. M. J. Razavi (razavismj@yahoo.com).

and apply only to electrically small apertures. Other formulations are derived from a power-balance method [5] and the widely quoted formula [6]. The other method for predicting the SE considers the enclosure as a waveguide and assuming only a single mode of propagation (the TE_{10} mode) [7]. On the other hand, the radiation from slots and apertures is usually decreased with electromagnetic gasketing and using very conductive and thick walls. In [8], the use of double-layered walls for shielded enclosures is proposed to increase the shielding effectiveness of them. The other method for optimizing the electromagnetic shielding rooms utilizes as minimum as possible absorbing materials on the inner surface of the rooms [9].

In this paper, a flexible and efficient way to analyze shielding rooms, especially with electrical large sizes and arbitrary shapes has been developed. The ray-tracing method has been applied to predict the Shielding Effectiveness (SE) of electromagnetic shielding rooms with apertures. The effect of metal cabinets and its position in the shielding effectiveness has been investigated.

2. MODELING TECHNIQUE

In the first step, the electric field in the electromagnetic shielding room is evaluated for a dipole antenna using the optimum ray-tracing method, described in Section 2.1. The next step explains the model of aperture which is often found on the walls of shielded rooms.

2.1. Optimum Ray-tracing Method

The known ray tracing technique which is based on geometrical optics (GO) provides a relatively simple solution for indoor wave propagation. It should be noted that using the GO and ray tracing technique is valid only when the object of interest has dimensions greater than the wavelength.

In the ray tracing method, the waves radiated from a transmitting antenna can be modeled as many ray tubes shooting from the location of the antenna [10, 11]. In a ray-tracing program, each ray tube may be composed of four rays separated by the increments of θ and φ ($\Delta\theta$ and $\Delta\varphi$) in local spherical coordinates, centered at the antenna. To generate the ray tubes, a sphere of radius r centered at the antenna is divided into quadrilateral cells that are close to squares with approximately the same area by selecting a fixed $\Delta\theta$ and a $\Delta\varphi = \Delta\theta / \sin\theta$. Fig. 1 shows the simulated region that is an electromagnetic shielding room with an aperture and a metal cabinet.

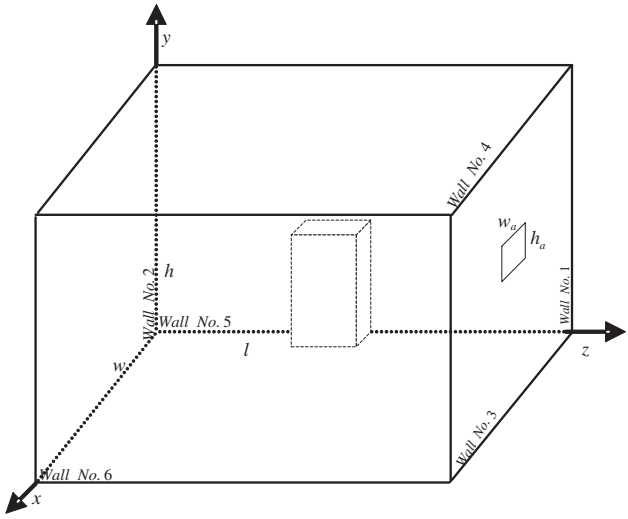

Figure 1. Geometry of an electromagnetic shielding room with an aperture and a metal cabinet.

In the conventional ray-tracing procedure, the rays have been traced one by one [10–12], taking a large run time. To speed up the ray tracing algorithm, we propose to trace the rays simultaneously. The computation time is reduced proportional to the number of considered rays. In this way, the ray-tracing procedure may be modified by the following seven steps:

1) Each ray of the ray tubes is traced to find an incident point (as shown in Fig. 2) where a ray propagates from a point $P_1(x_1, y_1, z_1)$ to an incident point $P_2(x_2, y_2, z_2)$ on an intercepting interface. The coordinates of the incident point P_2 can be determined from the following expression:

$$(x_2, y_2, z_2) = (x_1, y_1, z_1) + s\hat{s} \tag{1}$$

where $\hat{s}$ is the directional vector of the incident ray and s is the path length of the ray. For a flat interface defined with a normal unit vector $\hat{n} = (n_1, n_2, n_3)$ and a point $P_0 = (a, b, c)$ on the interface, the path length is given by

$$s = \frac{\hat{n} \cdot (P_0 - P_1)}{\hat{n} \cdot \hat{s}} \tag{2}$$

This is obtained from the equation $\overrightarrow{P_0P_2} \cdot \hat{n} = 0$. For a finite-size interface, it is also necessary to check whether the incident point is within the boundary of the interface or not. All interfaces

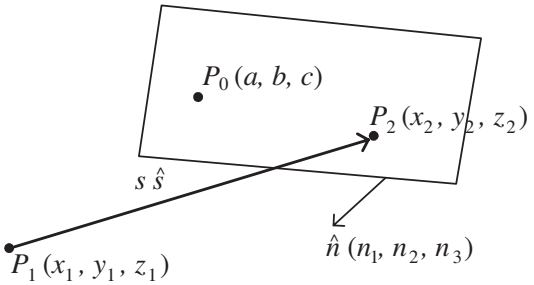

Figure 2. A ray propagates from P_1 to P_2 on an intercepting plane.

that may be illuminated by the ray tube should be tested to find the incident points and the incident point with the shortest path length from P_i is the true intercepting point. Except for the initial rays from the transmitting antenna, point P_1 is on an interface, too. Thus, for each interface that may start the ray tracing, based on the relative geometry of the structures, a list of the searching order over the other interfaces to find the incident point may be generated before starting the ray-tracing procedure to improve program efficiency.

2) When a ray tube incidents on an interface, a reflected and a transmitted ray tube is generated according to Snell's law and the local plane wave approximation. The reflection and transmission coefficients derived for a plane wave illuminating a flat interface of two materials are employed [13].

3) The boundary surfaces intersected with all rays have to be found at one time. Consider one of the boundary surfaces with a rectangular shape as shown in Fig. 3 whose normal unit vector is $\hat{n}_i$. One plane (Oa_ja_{j+1}), in which $j = 1, 2, 3, 4$, o is the point source and a_js are the edge points of the boundary surface, is passed through each side of this boundary surface $(\overline{a_ja_{j+1}})$ and the point source. The normal unit vector of each defined plane can be determined from the following expression:

$$\hat{n}_{ij} = \frac{\overrightarrow{oa_j} \times \overrightarrow{oa_{j+1}}}{|\overrightarrow{oa_j} \times \overrightarrow{oa_{j+1}}|} \tag{3}$$

A function f is defined such that it takes 1 for the rays incident to the boundary surface No. i and takes zero for the other rays [14].

$$f\,(i, \hat{r}) = 1 + \text{sign}\left(\sum_{\text{j=1}}^{4} \text{sign}\,(\hat{n}_{ij}.\hat{r}) - 4\right) \tag{4}$$

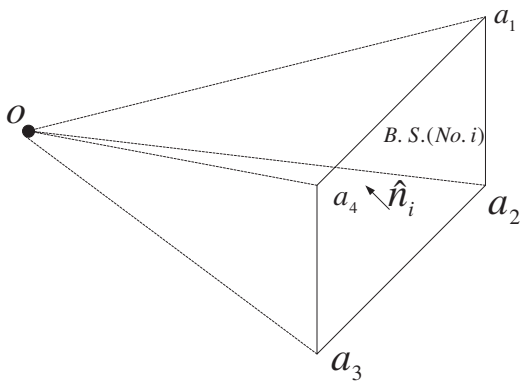

Figure 3. Boundary surface number i; $i = 1, 2, 4, 6$ and source point.

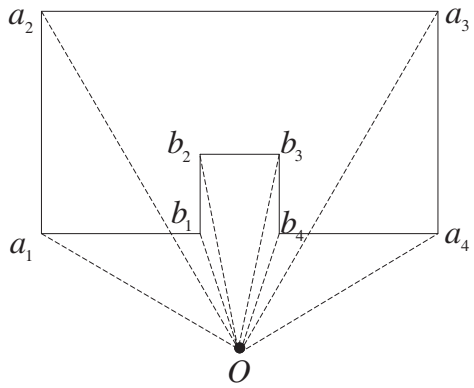

Figure 4. Boundary surface number i; $i = 3, 5$ and source point.

where $\hat{r}$ is directional vector of the incident ray and *sign* is the sign function. The function f for other surfaces with arbitrary shape as shown in Fig. 4 can be defined as the following expression:

$$f\left(i, \hat{r}\right) = 1 + \text{sign}\left(\sum_{\text{j=1}}^{8} \text{sign}\left(\hat{n}_{ij}.\hat{r}\right) - 8\right) \tag{5}$$

4) The sum of the products of defined functions f and the normal unit vectors $\hat{n}_i$ give us the normal unit vector of the corresponding boundary surfaces of all rays, at one time, as the following relation:

$$\hat{n} = \sum_{i=1}^{10} f\left(i, \hat{r}\right) \cdot \hat{n}_i \tag{6}$$

The simulated region as shown in Fig. 1 has ten boundary surface, six externally surface for shielding room and four internally surface for metal cabinet. Also, an arbitrary point of corresponding boundary surfaces of all rays can be found using a similar expression as follows:

$$P = \sum_{i=1}^{10} f\left(i, \hat{r}\right) \cdot P_i \tag{7}$$

where P_i is an arbitrary point on the intersecting boundary surfaces No. i.

5) A ray tube will be terminated if:
a) It exits outdoor or leaves the simulated domain;
b) The magnitude of the E-field is less than a threshold. For b), the total length of the ray paths from the transmitting antenna to the present location is used to approximate the spreading factor of the E-field. A convergence test should be performed to set the proper threshold, which is defined as the percentage of the reference field strength at 1 m from the transmitting antenna. If both the reflected and transmitted rays are significant, one of the ray tubes is stored by pushing it into a "stack," while the other one is continuously traced. The data set for each stored ray tube includes the directional vectors, positions, total path lengths, and E-field phasors (excluding the spreading factor) of the four rays. If both ray tubes are ended, a previously saved ray-tube data set is then popped from the stack and the ray-tracing procedure is started again. When the stack is empty, a new initial ray tube from the transmitting antenna is traced until finished. Multiple reflections and transmissions through walls, ceiling, stairs, floors, and other electrically large bodies can be simulated both in air and in the structures to properly model wave propagation and penetration in buildings.

6) In this work, the simulated domain is a rectangular enclosure with dimensions $w \times h \times l$ that contains a rectangular aperture with dimensions $w_a \times h_a$ as shown in Fig. 1. The aperture is meshed by using a rectangular grid with the square cells of the size $\Delta l_1 \times \Delta l_1$ that is given by:

$$\Delta l_1 = \frac{(l + w)}{N} \tag{8}$$

where N is the resolution factor of the ray tracing algorithm ,which is equal to $\pi/\Delta\theta$. The E-field matrix (with initial zero value) for this grid is considered. In each iteration of the ray tracing process, the E-field of the ray tubes which incident to the cells of the grid should be calculated and added to the initial E-field matrix.

7) In this work, transmission ray tubes leave the simulated domain and only reflection ray tubes are traced at each interface. From the geometrical optics, the E-field of the ray tube at the test point can be determined from the following equation:

$$\vec{E} = \vec{E}_0 \cdot \left\{ \prod \overline{\overline{R_i}} \right\} \cdot \left\{ \prod e^{-r_i l_i} \right\} \cdot SF \tag{9}$$

where $\vec{E}_0$ is the E-field at a reference point r_0, $\left\{ \prod \overline{\overline{R_i}} \right\}$ is the reflection coefficient dyad along the whole ray path, $\left\{ \prod e^{-r_i l_i} \right\}$ is the product of the propagation phase variations and exponential losses for this ray contribution starting from r_0, and SF is the spreading factor. By the conservation of energy flux in a ray tube [13], SF can be obtained by using

$$SF = \sqrt{A_0} \Big/ \sqrt{A} \tag{10}$$

where A_0 and A are the cross-sectional areas of the ray tubes at the reference point r_0 and the field point r, respectively. The sum of the areas of the four triangles on the intercepting quadrilateral at the receiving point as shown in Fig. 5 may be evaluated to approximate the cross-sectional area A.

It is worth mentioning that the proposed ray tracing algorithm could be useful in numerical software, such as MATLAB which based on matrix operations.

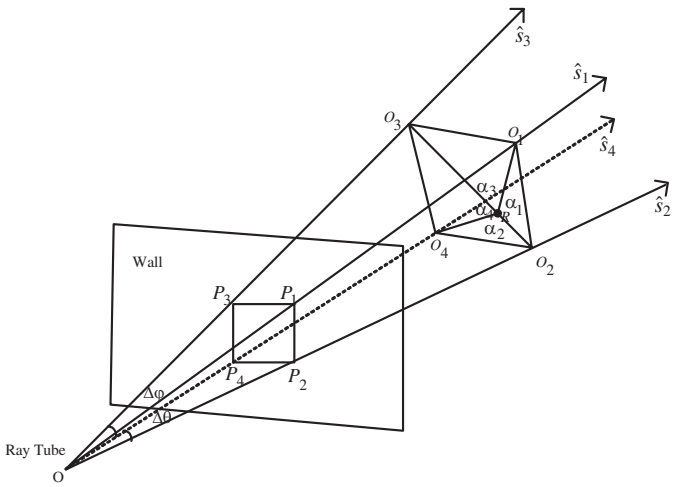

Figure 5. A ray tube passing a receiving antenna at R.

2.2. Leakage Field of Apertures

An aperture in the form of a slot, which is often found on the walls of shielded rooms, is usually analyzed as an aperture antenna mounted on an infinite ground plane. The electromagnetic penetration through an aperture depends on the distribution of tangential field components on the aperture surface $\vec{E}_a(r)$ calculated using the proposed algorithm in the previous subsection. The equivalent magnetic current density over aperture is equal to

$$\vec{M}(r) = 2\hat{n} \times \vec{E}_a(r) \tag{11}$$

where $\hat{n}$ is the normal vector of slot.

The fields radiated by the aperture can be expressed as [13]

$$\vec{E} = \frac{1}{4\pi} \iint_{S_a} \left[\hat{R} \times \vec{M}(r')\right] \frac{1 + j\beta R}{R^2} e^{-j\beta R} ds' \tag{12}$$

where $R = |r - r'|$ and the primed coordinate r' represents the source and the unprimed coordinate r represents the observation point and β is the propagation constant.

3. RESULTS

3.1. Validation

The proposed method is suitable only for the objects having dimensions greater than the wavelength of the source wave. Of course the results of applying this method to the small objects may be acceptable if the frequency range doesn't contain the resonance frequencies. Fig. 6 shows this matter for a 50 cm cubic box containing an aperture with dimensions 2 cm × 1 cm in the center of one of the walls. The simulation parameters are assumed $\Delta\theta = .5°$, $N = 360$ and $\Delta l_1 = 2.5$ mm. In this figure the results of proposed method have been compared with the results of Bethe approximation method [4]. The Bethe approximation method is valid only for the case when the aperture dimension less than wavelength. The excitation antenna is a Hertzian dipole located in the center of the box and the observation point is considered 3 m far from the center of the aperture on the z axis.

In order to evaluate the proposed method for large boxes, another example is presented. Consider a 3 m cubic box containing an aperture with dimensions 30 cm × 10 cm in the center of one of its walls. Also, the observation point is considered 3 m far from the center of the aperture on the z axis. The excitation antenna is a Hertzian dipole with the current magnitude I_0, located in the center of the box. The relative magnitude of E/I_0 has been calculated by the proposed method and

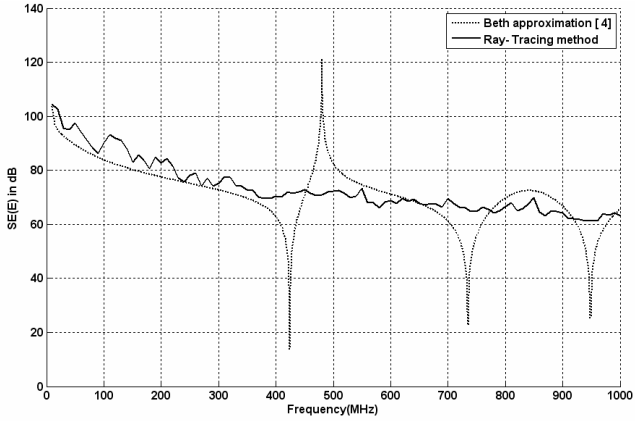

Figure 6. Comparison between the predicted $SE(E)$ by the ray-tracing method and Bethe approximation [4].

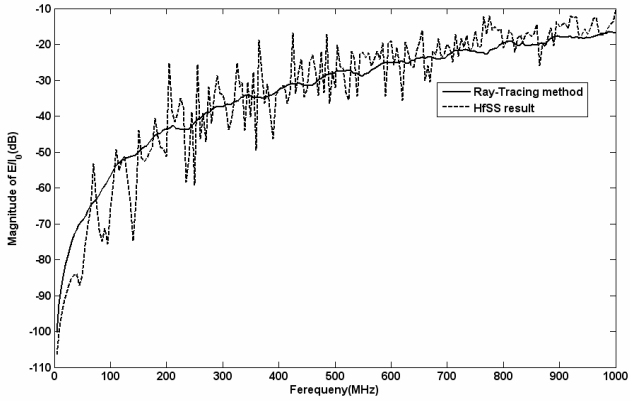

Figure 7. Comparison between predicted E/I_0 by the ray-tracing method and HFSS software.

compared with the results of HFSS11 full wave simulator in Fig. 7. The agreement between the results is good in the whole of frequency range especially in the high frequencies because the ray tracing method is an approximation technique for high frequency wave propagation.

3.2. Analyze the Main Problem

The proposed method has been applied to analyze the shielding room considered in the second example ($w = h = l = 3\,\text{m}$, $w_a = 30\,\text{cm}$,

$h_a = 10\,\text{cm}$) containing a metal cabinet with dimensions $30\,\text{cm} \times 150\,\text{cm} \times 75\,\text{cm}$. The simulation parameters are $\Delta\theta = 1.5°$, $N = 120$ and $\Delta l_1 = 5\,\text{cm}$. The $SE(E)$ has been calculated assuming the excitation antenna to be placed in the point $(1.5, 1.5, 1.5)$ (the center of shielding room) and the observation point to be $(1.5, 1.5, 6)$.

At the first example, a metal cabinet has been placed in position C as shown in Fig. 8 and investigated its effect in the shielding effectiveness of shielding room. The obtained results of this example are shown in Fig. 9. Adding metal cabinet to the shielding room in position C reduced the $SE(E)$. The reason is that the volume of the shielding room has been reduced and electromagnetic field to be forced out through aperture.

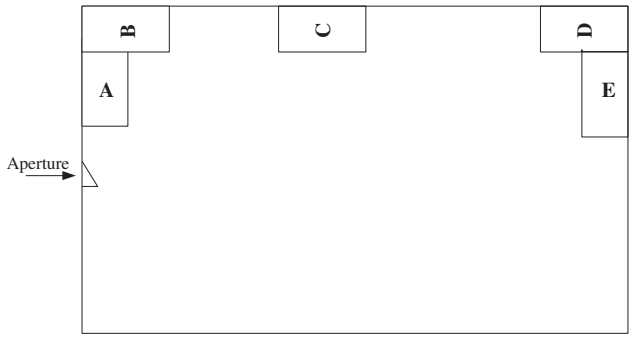

Figure 8. Top-view of the electromagnetic shielding room along with various positions of metal cabinet.

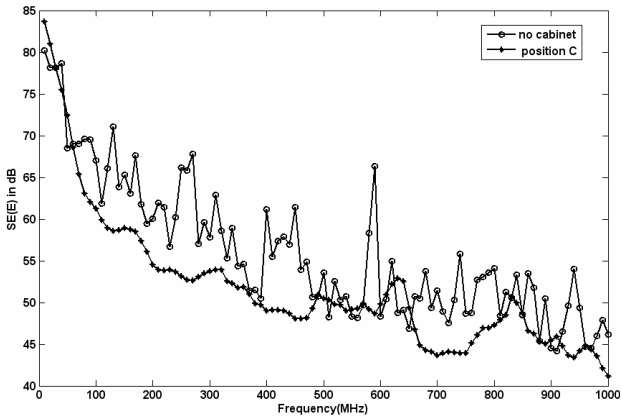

Figure 9. The predicted $SE(E)$ of the shielding room with and without the metal cabinet.

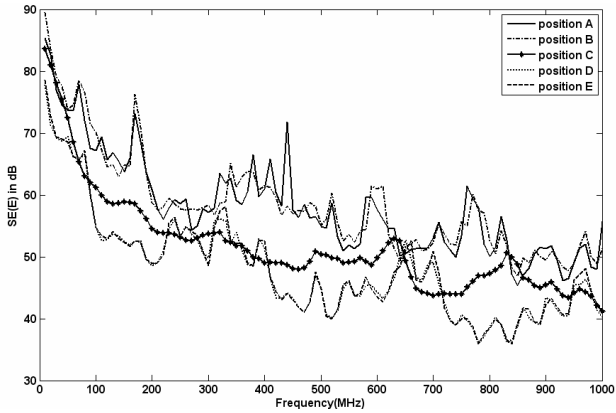

Figure 10. The predicted $SE(E)$ of the shielding room with and without the metal cabinet.

At the second example, the position of metal cabinet has been changed at several points A, B, C, D and E as shown in Fig. 8. The obtained results of this example are shown in Fig. 10. Undesired effect of the cabinet at positions A and B is less than other positions because these positions are not in line of site with the aperture. So the positions A and B are optimum.

4. CONCLUSION

In this paper, a fast and efficient method was proposed to analyze the electromagnetic shielding rooms with electrical large sizes and arbitrary shapes. The idea of this method is to trace all of the rays simultaneously in the ray tracing algorithm. The performance of the proposed method was verified by a comprehensive example. The effect of additional metal cabinet in the shielding effectiveness of shielding room was investigated. Also the position of it was found optimally to produce a "best" performance for the shielding room.

REFERENCES

1. Kraft, C. H., "Modeling leakage through finite apertures with TLM," *IEEE Int. Symp. Electomagn. Campat.*, 73–76, Chicago, IL, Aug. 1994.
2. Martin, T., M. Bäckström, and J. Lorén, "Semi-empirical modeling of apertures for shielding effectiveness simulations," *IEEE Trans. Electroman. Compat.*, Vol. 45, No. 2, 229–237, May 2003.

3. Bunting, C. F. and S.-P. Yu, "Field penetration in a rectangular box using numerical techniques: An effort to obtain statistical shielding effectiveness," *IEEE Trans. Electroman. Compat.*, Vol. 46, No. 2, 160–168, May 2004.
4. Wallyn, W., D. De Zutter, and E. Laerman, "Fast shielding effectiveness prediction for realistic rectangular enclosures," *IEEE Trans. Electomagn. Campat.*, Vol. 45, 639–643, Nov. 2003.
5. Marvin, A. C., J. F. Dawson, S. Ward, L. Dawson, J. Clegg, and A. Weissenfeld, "A proposed new definition and measurement of the shielding effect of equipment enclosures," *IEEE Trans. Electomagn. Campat.*, Vol. 46, No. 3, 459–468, Aug. 2004.
6. Ott, H. W., *Noise Reduction Techniques in Electronic Systems*, 2nd Edition, Wiley, New York, 1988.
7. Robinson, M. P., T. M. Benson, C. Christopoulos, J. F. Dawson, M. D. Ganley, A. C. Marvin, S. J. Porter, and D. W. P. Thomas, "Analytical formulation for the shielding effectiveness of enclosures with apertures," *IEEE Trans. Electomagn. Campat.*, Vol. 40, No. 3, 240–247, Aug. 1998.
8. Razavi, S. M. J. and M. Khalaj-Amirhosseini, "Using double-layers walls for shielded enclosures," *Microwave Conference Proceedings, APMC 2005. Asia-Pacific Conference Proceedings*, Vol. 2, No. 4–7, Dec. 2005.
9. Razavi, S. M. J. and M. Khalaj-Amirhosseini, "Optimum design of electromagnetic shielding rooms with minimum usage of absorbing materials," *International Journal of RF and Microwave Computer Aided Engineering*, Vol. 20, No. 1, Jan. 2010.
10. Yang, C.-F., B.-C. Wu, and C.-J. Ko, "A ray-tracing method for modeling indoor wave propagation and penetration," *IEEE Trans. Antennas Propagat.*, Vol. 46, No. 6, 907–919, Jun. 1998.
11. Kim, H. and H. Ling, "Electromagnetic scattering from an inhomogeneous object by ray tracing," *IEEE Trans. Antennas Propagat.*, Vol. 40, 517–525, May 1992.
12. Razavi, S. M. J. and M. Khalaj-Amirhosseini, "Optimization of an anechoic chamber with ray-tracing and genetic algorithms," *Progress In Electromagnetics Research B*, Vol. 9, 53–68, 2008.
13. Balanis, C. A., *Advanced Engineering Electromagnetics*, Wiley, New York, 1989.
14. Razavi, S. M. J., M. Khalaj-Amirhosseini, and A. Cheldavi, "Minimum usage of ferrite tiles in anechoic chambers," *Progress In Electromagnetics Research B*, Vol. 19, 367–383, 2010.